ISSN 0915-633X

NATIONAL INSTITUTE FOR FUSION SCIENCE

Effect of Alpha Particles on Radial Electric Field Structure in Torsatron/Heliotron Reactor

K. Itoh, H. Sanuki and S.-I. Itoh

(Received – Aug. 31, 1992)

NIFS-182 Sep. 1992

RESEARCH REPORT
NIFS Series

NAGOYA, JAPAN

Effect of Alpha Particles on Radial Electric Field Structure in Torsatron/Heliotron Reactor

K. Itoh, H. Sanuki

National Institute for Fusion Science, Nagoya, 464-01, Japan

and S.-I. Itoh

Research Institute for Applied Mechanics, Kyushu University 87
Kasuga 816, Japan

Abstract

The radial electric field structure in the fusion reactor of the Torsatron/Heliotron configuration is discussed taking into account the effects of the orbit loss of α particles. It was found that the direct loss of α-particles has small influence on the profile of the radial electric field. The trapping efficiency of the alpha particle is also evaluated by using the self-consistent radial electric field.

Keywords: Helical System, Reactor Plasma, Alpha Particle, Radial Electric Field, Loss Cone Loss

§1 Introduction

Recently, it has been widely recognized that the radial electric field E_r plays an important role on the confinement in helical devices (stellarators) such as Torsatron/Heliotron configurations(Gourdon, et al., 1968; Mohri, 1970; Uo, 1971). In Torsatron/ Heliotron stellarators, the neoclassical theory predicts that an electric field reduces the helical ripple loss and improves the confinement(Furth, et al., 1968; Hastings, et al., 1985). The detailed measurement of the electric field and their effects on confinement has been one of the key topics in helical systems.

In the Wendelstein VII-A (WVII-A) stellarator(Wobig, et al, 1987) and Heliotron-E (Kondo, et al., 1988) devices, E_r near edge was measured. It has been found that a large negative electric field ($E_r \sim -450$V/cm) was built up by the fast ion loss of perpendicularly-injected neutral beams in WVII-A. We have developed the self-consistent analyses on the loss and E_r to evaluate the heating efficiency by energetic particles(Itoh, et al., 1992a; Sanuki, et al., 1991). Quantitative comparison of the theory and experiments on E_r profiles is made, and the influence of the direct ion loss has been identified(Itoh, et al., 1992a, 1992b). The analyses on the CHS experiment(Ida, et al., 1992) has shown that the direct loss of NBI particle has small effect, except the plasma periphery region(Sanuki, 1991, 1992). These analyses have clarified that (1)there is a strong mutual interaction between the loss cone loss and radial electric field, and

(2) the mutual influence depends on the plasma parameter as well as the geometry. The application of this method for future burning plasmas is necessary, since the absolute trapping of the fusion products, α-particle in DT reactor, is the important issue for evaluating the prospect of the helical reactor. A significant role of the radial electric field on the confinement in a reactor grade plasma was confirmed (Watanabe, 1992). The determination of the self-consistent determination is an important issue.

In this article, we apply a theoretical model to the reactor grade plasmas, in order to determine the radial electric field and direct loss of α-particles simultaneously. The roles of the α-particle loss on E_r are investigated. It is found that there is a large contribution from the neoclassical process and α-particle has only small effect on E_r. The ratio of the direct loss is calculated by using the self-consistent radial electric field.

§2 The Model

The model geometry is chosen such that the magnetic field structure is fitted to the conventional torsatron configuration with one helical harmonic, to simplify the following analysis, as

$$B = B_0[1-\varepsilon_t(r)\cos\theta-\varepsilon_h(r)\cos(\ell\theta-m\phi)], \tag{1}$$

$$\varepsilon_t(r) = r/R, \tag{2-1}$$

and

$$\varepsilon_h(r) = \ell\varepsilon_0 I_\ell(mr/R), \tag{2-2}$$

where m is the toroidal pitch number, ℓ is the multipolarity, I_ℓ is a modified Bessel function of the first kind. r and R are the minor and major radius, respectively. This simplification gives the form of the rotational transform ι as

$$\iota(r) = \frac{\ell^3 R}{2r} \varepsilon_0{}^2 \frac{d}{dx} \left[\frac{I_\ell I_\ell'}{x}\right] \tag{3}$$

where x=mr/R, ' ≡d/dx, and the safety factor is given by $q(r)=1/\iota$. The modulation of the helical winding (Nishimura, 1990) is often introduced, which is characterized by the parameter α_*. The effect of α_* was examined (Ida, et al., 1992); it was confirmed that the α_* effect changes E_r only slightly.

We study the steady state solution of the ambipolarity equation, taking into account nonclassical terms in the particle flux Γ as

$$\Gamma_i = \Gamma_i^{NC(s)} + \Gamma_i^{NC(as)} + 2\Gamma_\alpha. \tag{4-1}$$

This equation consists of the neoclassical fluxes (denoted by the superscript of NC) of bulk ions and the orbit loss flux of α-particles (Γ_α). The charge exchange process can influence the radial electric field (Ohkawa, 1986; Sanuki, 1991, 1992). This process is neglected here in order to study the mutual influence of α-particle loss and E_r. The orbit loss of bulk ions are not taken into account, because the bulk ions are not in the collisionless regime for the discharges of our interest. The neoclassical contribution is given as the sum of the flux $\Gamma_i^{NC(s)}$, associated with the passing and toroidally trapped particles, and $\Gamma_i^{NC(as)}$ related to the ripple trapped particles. We use a formula by Kovrizhnykh (Kovrizhnykh, 1984). For electrons, the nonclassical terms in Eq.(4-1) are insignificant. Only the neoclassical terms are kept in the electron flux as

$$\Gamma_e = \Gamma_e^{NC}. \tag{4-2}$$

The explicit form of the α-particle orbit loss is given as

$$\Gamma_\alpha(r) = \frac{1}{r}\int_{r_*}^{r} \sqrt{2\varepsilon_h}\, S_\alpha r\, dr, \tag{5}$$

where S_α is the birth rate of α-particle per unit volume and is P_α/W_α, (P_α is the α-power density and W_α denotes the α-particle energy,) and r_* is the radius representing the loss boundary. In this article, we estimate r_* by that for the deeply trapped particle. The average with respect to the pitch angle is approximated by $\sqrt{2\varepsilon_h}$. This estimation is slightly underestimating, but does not change the conclusion of this article. The loss cone region is a functional of the radial electric field. The dependence of the radius r_* on the radial electric field was discussed and its expression is given (Itoh, et al., 1991).

The source rate S_α is calculated once the fusion cross section is given:

$$S_\alpha = \frac{1}{4} n_e{}^2 \langle \sigma v \rangle (1 - f_d)^2 \qquad (6)$$

where n is the electron density, $\langle \sigma v \rangle$ is the fusion cross section, and f_d is the dilution factor of fuels by impurities, $\Sigma Z_I n_I / n_e$ (suffix I stands for impurities). The DT mix ratio n_D/n_T is chosen to be unity. For the analytic study, we employ the fitting formula of $\langle \sigma v \rangle$ as (Takizuka, et al., 1987)

$$\langle \sigma v \rangle = 3.7 \times 10^{-18} T_i{}^{-2/3} \exp\{-20 T_i{}^{-1/3}\}/h \quad (m^3/s) \qquad (7\text{-}1)$$

$$h = T_i/37 + 5.45/[3 + T_i\{1 + (T_i/37.5)^{2.8}\}] \qquad (7\text{-}2)$$

where T_i is measured in a unit of keV.

The radial electric field solution in the steady state is evaluated by the ambipolarity equation

$$\Gamma_i = \Gamma_e. \qquad (8)$$

This equation determines E_r, the ambipolar particle flux Γ, and the loss cone region r_*, simultaneously.

Equation (8) is a nonlinear algebraic equation with respect to the radial electric field. Equation (8) can have multiple solutions on each magnetic surface. It should be noted that this equation is given on each magnetic surface, and contains a class of solutions $E_r(r)$ which have discontinuities at some radial points. The fundamental solution to the problem of the discontinuity can be given by noticing the small but finite diffusion coefficient of the radial electric field (Yahagi, et al., 1988). We look for the solution which is continuous and satisfies the condition

$$E_r(r) \rightarrow 0 \text{ as } r \rightarrow 0. \tag{9}$$

§3 Radial Electric Field and Direct Loss of α-Particles

We estimate the radial electric field from the ambipolar condition Eq.(8). Two cases are selected for the machine parameters as shown in Table I. In case [A], large size is chosen. Case [B] is for a design of small machines size. The plasma profiles are chosen to be parabolic as

$$n_e(\rho) = \{n(0)-n_s\}\{1-\rho^2\} + n_s \tag{10}$$

and

$$T_{e,i}(\rho) = \{T(0)-T_s\}\{1-\rho^2\} + T_s, \tag{11}$$

where ρ is the normalized radius r/a. We choose, in the following calculations, the parameters of $n(0) = 5\times10^{20}/m^3$, $n_s = 10^{19}/m^3$ and T_s =200eV, unless otherwise specified. High density parameter is chosen, because the neoclassical energy loss can be more serious for the case of low density operations.

(3.1) Radial Electric Field Structure

Figure 1 shows the self-consistent solution of the radial electric field profile for case [A] for various values of T(0). Negative radial electric field is obtained, which reaches of the order of -40kV/m for the case of T(0)=25keV. The radial electric field becomes more negative in proportion to the temperature. This electric field is influenced by the direct loss of α-particles very little. Figure 2 shows the result of the case [B]. Negative radial electric field of the similar magnitude is obtained. It is also noted that the electric field starts to approach to zaro or positive value, near the edge, at high temperature cases. This is because the electron loss becomes more important.

In these calculations, the loss cone of α-particle and the radial electric field are determined self-consistently. It is found that the electric field has weaker dependence on the temperature. Figure 3 illustrates Γ_α and Γ_i^{NC} at ρ=0.5 and 0.7 as a function of T(0). (Solid lines are for the values at ρ=0.7 and dashed lines at ρ=0.5 for the α-particle flux and the neoclassical flux Γ^{NC}.) It is clearly shown that the net particle flux is dominated by the contribution of the bulk particles. Figure 4 is for the case [B] and the same conclusion is obtained. It is noted that the ratio $\Gamma_\alpha(\rho=0.7)/\Gamma_\alpha(\rho=0.5)$ is an increasing function of T(0). This is because the birth profile becomes more broader for higher temperature case as is understood from Eq.(7). This T(0) dependence is stronger for the case [B] compared to the case [A], because the loss cone region is narrower for [B] in the absence of E_r effects.

We note the dependence of Γ_j^{NC} on E_r. Figure 5 shows Γ^{NC} for electrons and ions at ρ=0.5 and 0.7 for the case of T(0)= 10keV. For both cases, the derivative of Γ_i^{NC} with respect to E_r, $\partial\Gamma_i^{NC}/\partial E_r$, is much larger than that for electrons $\partial\Gamma_e^{NC}/\partial E_r$, for the present parameters. This indicates that the additional α-particle flux is not effective in affecting the solution of E_r. The relation $\Gamma_i^{NC} \simeq 0$ is a good approximate form in determining E_r. The influence of the additional α-particle fluxes Γ_α on the change of the radial electric field, ΔE_r, is estimated by the relation

$$\Gamma_\alpha \simeq -\Delta E \;\; \partial\Gamma_i^{NC(as)}/\partial E_r \tag{12}$$

where ΔE represents the difference of E_r between the neoclassical calculation and that with α-particle contribution.

(3.2) Direct Loss of α-Particles

The loss rate of α-particles is calculated selfconsistently. Figure 6 illustrates the loss cone region in the plane of r/a and the potential difference $\Delta\Phi \equiv \Phi(0)-\Phi(a)$ for cases [A] and [B]. The region between two lines (denoted by the symbol L) corresponds to the loss region. The solid line indicates the result of the self-consistent calculation, where the static potential is derived from the solution of Eq.(8). The dashed line shows the case of the simple estimation, where the radial shape of $\phi(r)$ is modelled by the parabolic shape. (It is found that, in the parameter region of this article, the approximation by the parabolic model gives a good approximation so long as to evaluate the loss cone boundary.)

Figure 7 shows the loss rate as a function of T(0). Loss rate is defined as ,

$$\eta_{loss} = 4\pi^2 aR\Gamma_\alpha(a)/\{\int S_\alpha dV\}. \tag{13}$$

When the influence of the radial electric field on the α-particle orbit is small, (i.e., T(0) is low in this case,) the case [A] has wider loss cone than the case [B] (as is understood from the difference of $\varepsilon_h/\varepsilon_t$) and has larger loss rate η_{loss}. The loss rate is an increasing function of the temperature. This has two reasons. First, when the temperature is low, $\langle\sigma v\rangle$ has a strong temperature dependence, and the fusion reaction is localized near the axis. As temperature increases, the birth profile becomes broader so that the direct loss increases. Secondly, as the temperature increases, the potential difference becomes larger as is shown in Figs.1 and 2. By this stronger negative radial electric field, the loss cone region becomes wider, as is illustrated in Fig.6. The loss rate is in the range of 25-30%.

§4 Summary and Discussion

In this paper, we applied the analytical method to model the effect of the direct loss of α-particles on the radial electric field and to determine the loss cone self-consistently to the reactor-grade plasma in torsatron/heliotron configurations. We examined the radial electric field profile and the loss cone loss of the fusion product α-particles self-consistently.

We confirmed that the orbit loss of fusion product has small effect on E_r compared to the neoclassical prediction. The large enhancement of the radial electric field, and hence the strong improvement of the confinement, by the direct loss of the α-particles, is not expected. The ratio of the absolute trapping of the energetic α-particle is also evaluated by using this electric field structure. It is about 70% for large and small designs of reactors.

The calculation in this article is done without considering other constraints such as the β-limit or the power amplification factor Q. For the case [A], β-value at the axis exceeds 40% at the temperature of 20keV. This is because we have chosen high density case. If one reduces the density and fixes T, Γ_α is reduced by the factor n^2, but Γ_i^{NC} reduces less. As a result of this, the influence of α-particle on the self-consistent radial electric field is weaker than this evaluation. From Figs.3 and 4, it is understood that the neoclassical energy fluc is considerably large compared to the α-particle heating. The expected Q-value would not be high, but this is beyond the scope of the article.

It should be noted that, in order to establish the reliability of the prediction in this article, a satisfactory explanation for the present experiments awaits further theoretical and experimental studies. The model of E_r profile based on Eq.(8) may be subject to change by the future progress. The improvement of the modelling for the present experimental plasmas is an urgent task in order to obtain the accurate estimation for the fusion plasmas.

Acknowledgements

Authors acknowledge discussions with Drs. A. Fukuyama, T. Takizuka and M. Fujiwara. This work is partly supported by the Grant-in-Aid for Scientific Research of MoE Japan.

References

Furth, H. P. and M. N. Rosenbluth, (1968): Plasma Physics and Controlled Nuclear Fusion Research (IAEA, Vienna) Vol.1, p821.

Gourdon, C., et al., (1968): Plasma Physics and Controlled Nuclear Fusion Research (IAEA, Vienna) Vol.1, p847.

Hastings, D. E., W. A. Houlberg and K. C. Shaing, (1985): Nucl. Fusion **25** 445.

Ida, K., H. Yamada, H. Iguchi, et al., (1992): Phys. Fluids **B4** 1360.

Itoh, K., H. Sanuki, J. Todoroki, et al., (1991): Phys. Fluids **B3** 1294.

Itoh, K., H. Sanuki, S.-I. Itoh, (1992a): Nucl. Fusion **32** 1047.

Itoh, K., H. Sanuki, S.-I. Itoh (1992b): J. Phys. Soc. Jpn. **61** in press.

Kondo, K., H. Zushi, S. Nishimura, et al., (1988): Rev. Sci. Instrum. **59** 1533.

Kovrizhnykh, L. M. (1984): Nucl. Fusion **24** 435.

Mohri, A. (1970): J. Phys. Soc. Jpn. **28** 1549.

Nishimura, K., et al. (1990): Fusion Technology, **17** 86.

Ohakawa, T. (1986): Kakuyuugou Kenkyuu **56** 274.

Sanuki, H., K. Itoh, K. Ida, S.-I. Itoh, (1991): J. Phys. Soc. Jpn. **60** 3698.

Sanuki, H., K. Itoh, and S.-I. Itoh (1992): Research Report NIFS-160 'Effects of Nonclassical Ion Losses on Radial Electric Field in CHS Torsatron/Heliotron' (National Inst. Fusion

Science).

Takizuka, T. and M. Yamagiwa (1987): JAERI-M 87-066 'Reactivity of DT plasma with beam induced tail in magnetic confinement system'.

Uo, K. (1971): Plasma Physics **13** 243.

Watanabe, K., et al (1992): J. Phys. Soc. Jpn. **61**, 863.

Wobig, H., H. Maassberg, H. Renner, The WVII-A Team, (1986): in Plasma Physics and Controlled Nuclear Fusion Research 1986, Proc. 11th Int. Conf. Kyoto, 1986 (IAEA Vienna) Vol.2, p369.

Yahagi, E., K. Itoh, M. Wakatani, (1988): Plasma Physics and Controlled Fusion **30** 1009.

Table I

	[A]	[B]
R(m)	20	7
a(m)	2	1
B(T)	4	5
m	10	10
ℓ	2	2
$\varepsilon_h(a)$	0.11	0.24
$\varepsilon_t(a)$	0.10	0.14

Figure Captions

Fig.1 Self-consistent solution of the radial profiles of the electric field for the case [A] are shown for the various values of T(0). Other parameters are chosen as $n(0)=5\times10^{20}m^{-3}$, $n_s=10^{19}m^{-3}$, and $T_s=200eV$.

Fig.2 Self-consistent solution of the radial profiles of the electric field for the case [B] are shown for the various values of T(0). Other parameters are chosen as $n(0)=5\times10^{20}m^{-3}$, $n_s=10^{19}m^{-3}$, and $T_s=200eV$.

Fig.3 α-particle flux and the ambipolar flux (Γ_α and Γ^{NC}) are shown as a function of T(0) for the case of [A]. Solid lines for $\rho=0.7$ and dashed lines for $\rho=0.5$ Other parameters are chosen as $n(0)=5\times10^{20}m^{-3}$, $n_s=10^{19}m^{-3}$, and $T_s=200eV$.

Fig.4 α-particle flux and the ambipolar flux (Γ_α and Γ^{NC}) are shown as a function of T(0) for the case of [B]. Solid lines for $\rho=0.7$ and dashed lines for $\rho=0.5$ Other parameters are chosen as $n(0)=5\times10^{20}m^{-3}$, $n_s=10^{19}m^{-3}$, and $T_s=200eV$.

Fig.5 Neoclassical fluxes Γ_e^{NC} (solid lines) and Γ_i^{NC} (dashed lines) are shown a function of E_r for $\rho=0.7$ and 0.5. Parameter are those for the case [B], T(0)=10keV and

$n(0)=5\times10^{20}m^{-3}$.

Fig.6 Loss cone boundary for deeply trapped particles for cases [A] and [B]. The region between two lines is the loss cone region. Solid line indicates the result where the potential shape of the self-consistent calculation of the radial electric field (case of T(0)=10keV) is used. The dashed line is for the case with the parabolic approximation for the static potential, $\phi(r)$. Here we use $W_\alpha=3.7MeV$, and $\Delta\Phi\equiv\phi(0)-\phi(a)$.

Fig.7 Ratio of the direct loss of α-particles as a function of T(0). Solid line is for [A] and dashed line is for [B]. Other parameters are chosen as $n(0)=5\times10^{20}m^{-3}$, $n_S=10^{19}m^{-3}$, and $T_S=200eV$.

Fig. 1

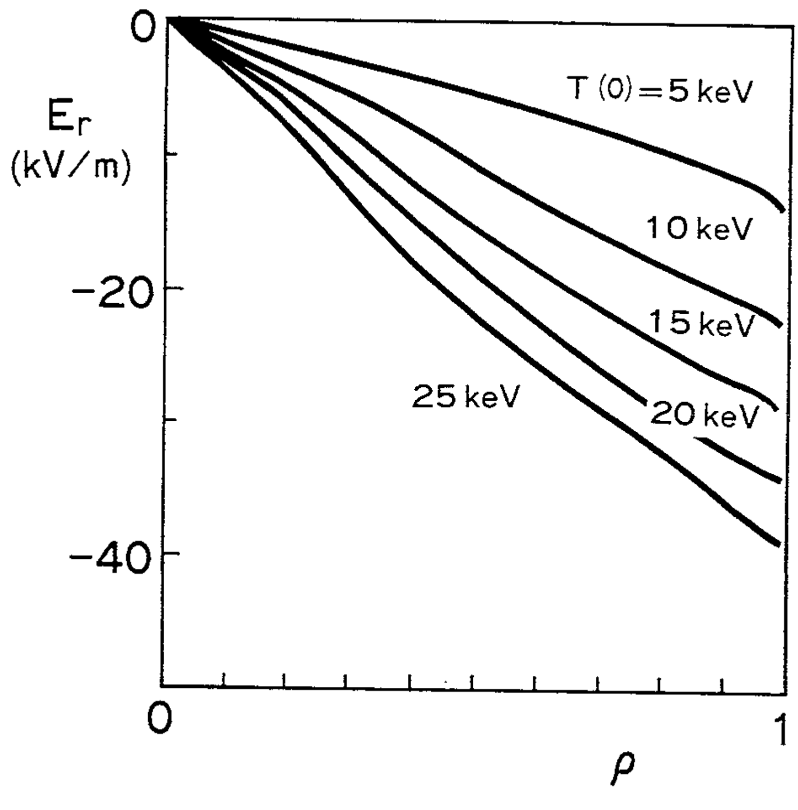

Fig. 2

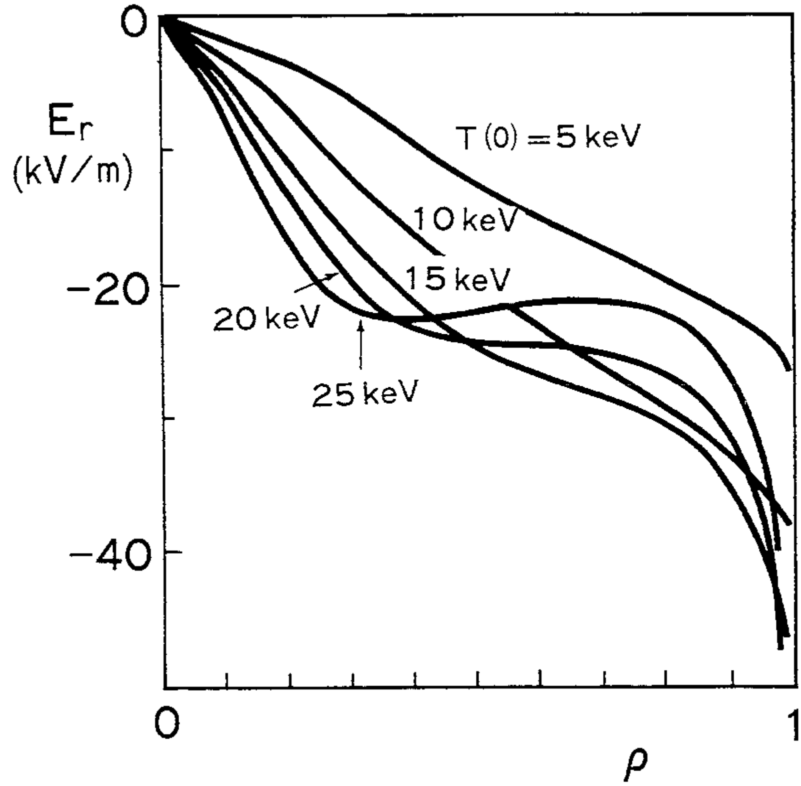

Fig. 3

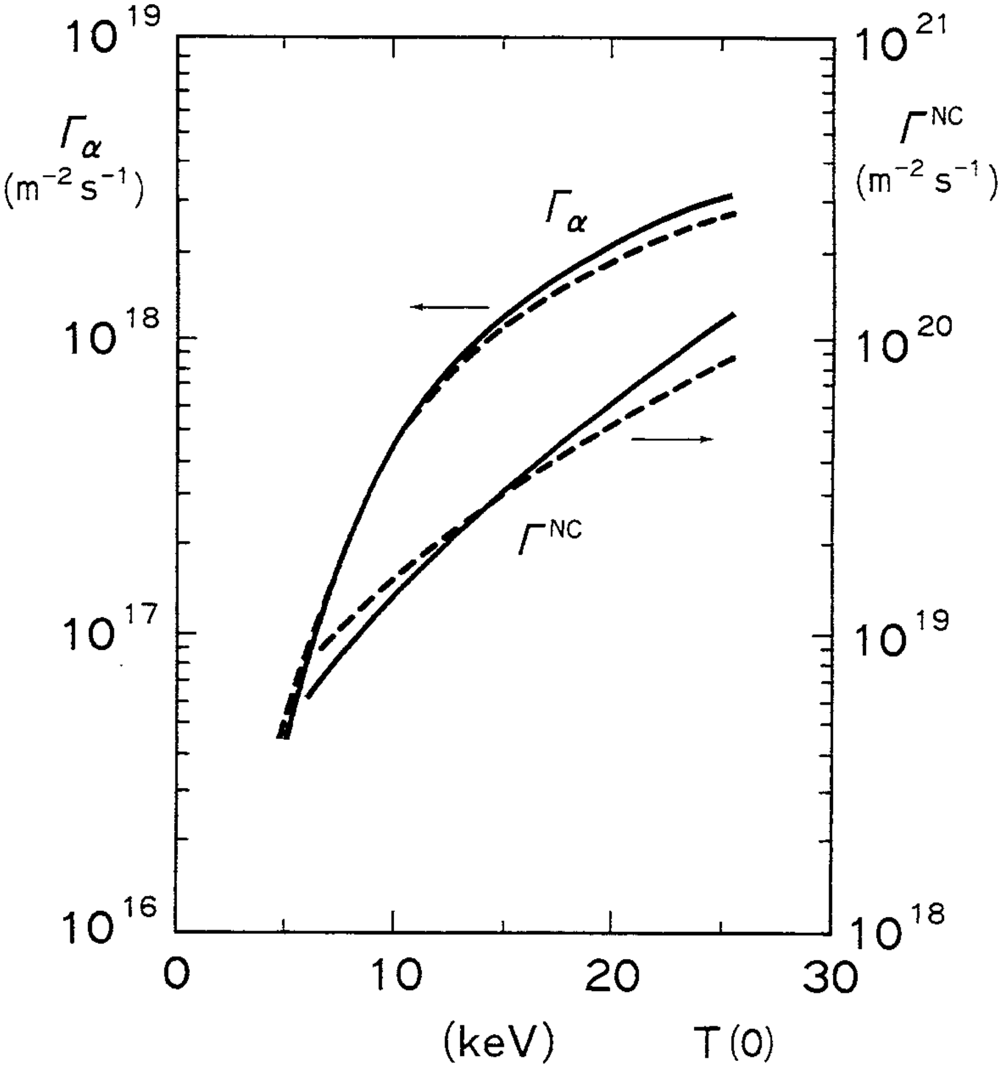

10^{19}
Γ_α
$(m^{-2}s^{-1})$
10^{18}
10^{17}
10^{16}
10^{21}
Γ^{NC}
$(m^{-2}s^{-1})$
10^{20}
10^{19}
10^{18}
Γ_α
Γ^{NC}
0
10
20
30
(keV)
T(0)

Fig.4

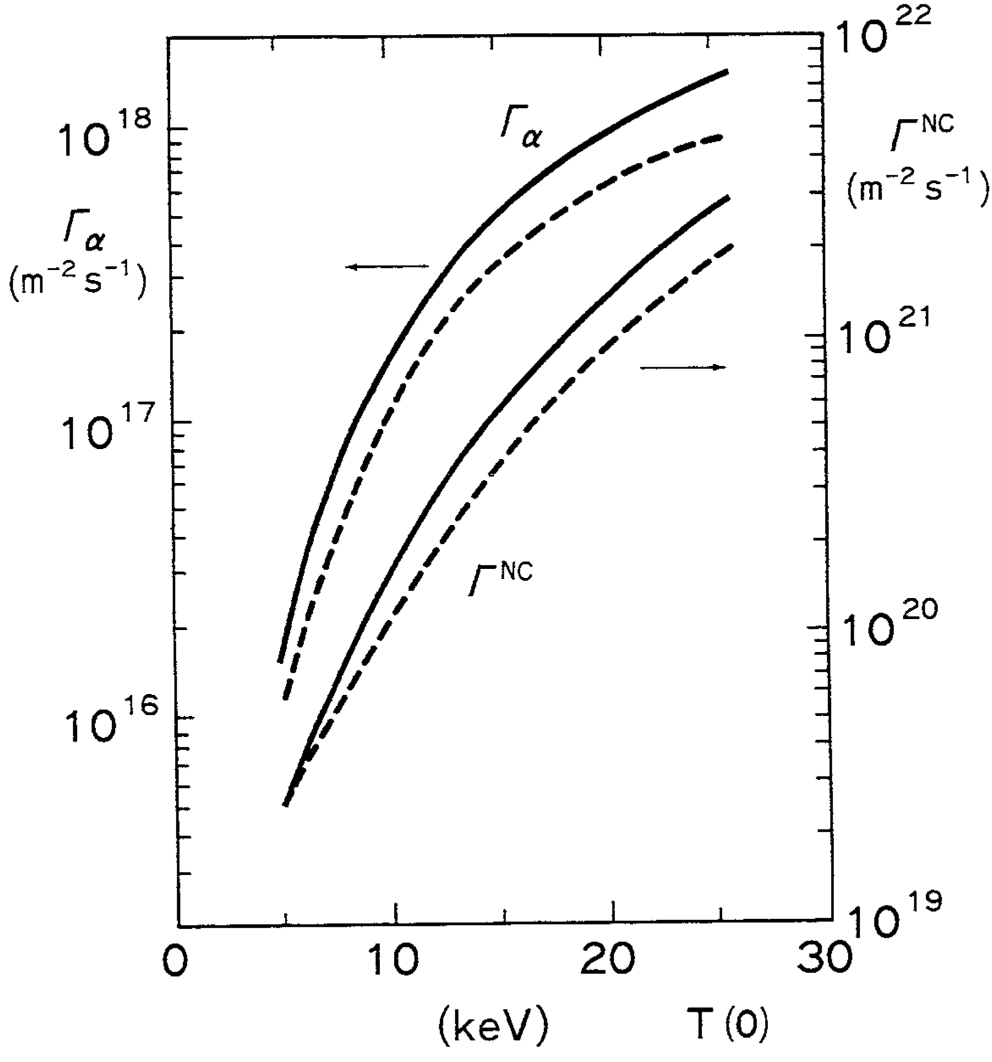

10^{18}
10^{17}
10^{16}
Γ_α ($m^{-2}s^{-1}$)
Γ_α
Γ^{NC}
10^{22}
10^{21}
10^{20}
10^{19}
Γ^{NC} ($m^{-2}s^{-1}$)
0
10
20
30
(keV)
T(0)

Fig.5

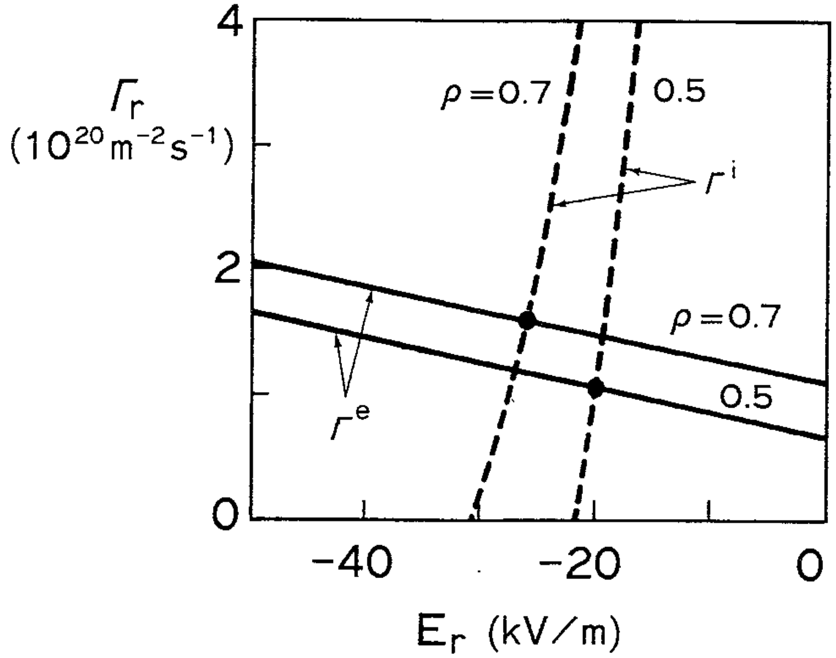

4
2
0
Γ_r
$(10^{20} m^{-2} s^{-1})$
$\rho = 0.7$
0.5
Γ^i
$\rho = 0.7$
0.5
Γ^e
-40
-20
0
E_r (kV/m)

Fig.6

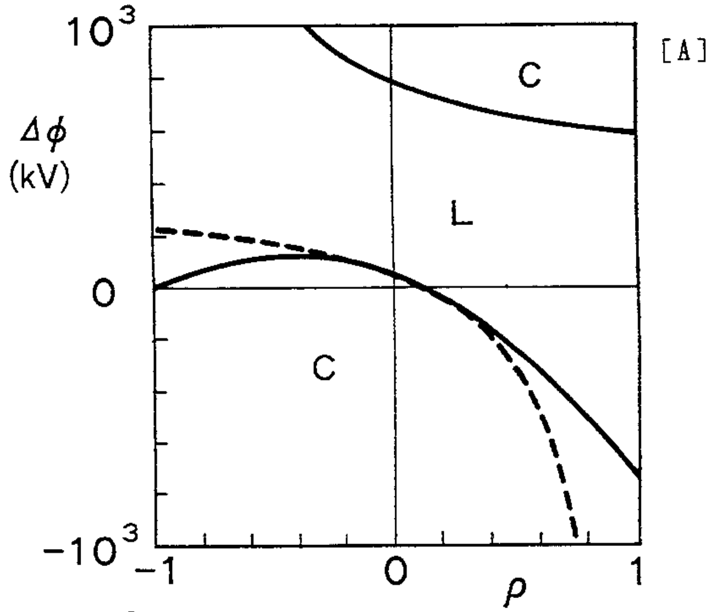
[A]
10^3
$\Delta\phi$
(kV)
C
L
0
C
-10^3
−1
0
1
ρ

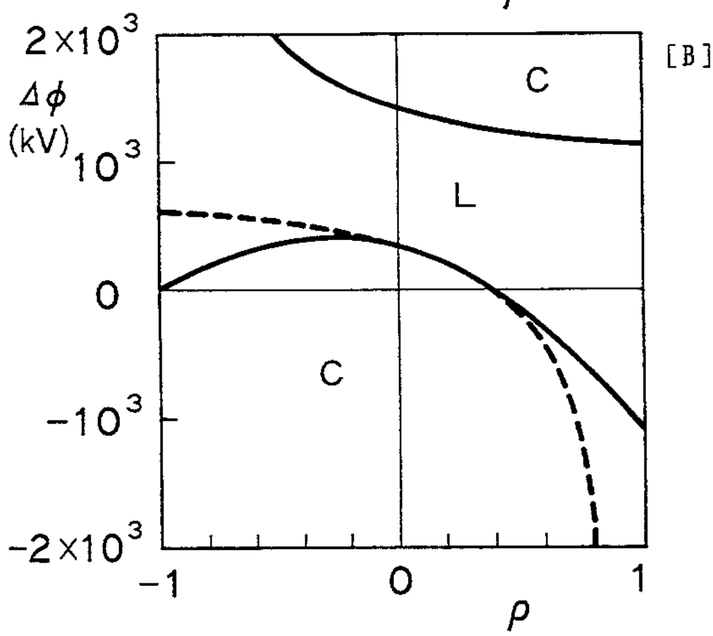
[B]
2×10^3
$\Delta\phi$
(kV)
10^3
C
L
0
C
-10^3
-2×10^3
−1
0
1
ρ

Fig.7

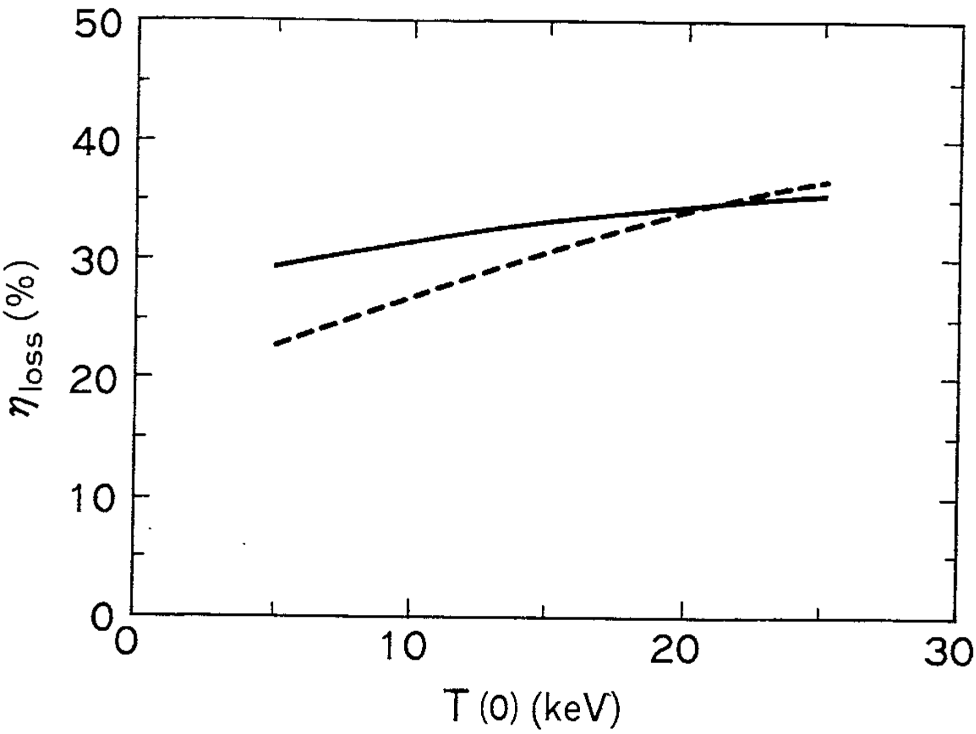

Recent Issues of NIFS Series

NIFS-135 H. Ji, H. Toyama, A. Fujisawa, S. Shinohara and K. Miyamoto *Fluctuation and Edge Current Sustainment in a Reversed-Field-Pinch;* Feb. 1992

NIFS-136 K. Sato and F. Miyawaki, *Heat Flow of a Two-Electron-Temperature Plasma through the Sheath in the Presence of Electron Emission;* Mar. 1992

NIFS-137 T. Hayashi, U. Schwenn and E. Strumberger, *Field Line Diversion Properties of Finite β Helias Equilibria;* Mar. 1992

NIFS-138 T. Yamagishi, *Kinetic Approach to Long Wave Length Modes in Rotating Plasmas*; Mar. 1992

NIFS-139 K. Watanabe, N. Nakajima, M. Okamoto, Y. Nakamura and M. Wakatani, *Three-dimensional MHD Equilibrium in the Presence of Bootstrap Current for Large Helical Device (LHD)*; Mar. 1992

NIFS-140 K. Itoh, S. -I. Itoh and A. Fukuyama, *Theory of Anomalous Transport in Toroidal Helical Plasmas;* Mar. 1992

NIFS-141 Y. Kondoh, *Internal Structures of Self-Organized Relaxed States and Self-Similar Decay Phase;* Mar. 1992

NIFS-142 U. Furukane, K. Sato, K. Takiyama and T. Oda, *Recombining Processes in a Cooling Plasma by Mixing of Initially Heated Gas*; Mar. 1992

NIFS-143 Y. Hamada, K. Masai, Y. Kawasumi, H. Iguchi, A. Fijisawa and JIPP T-IIU Group, *New Method of Error Elimination in Potential Profile Measurement of Tokamak Plasmas by High Voltage Heavy Ion Beam Probes;* Apr. 1992

NIFS-144 N. Ohyabu, N. Noda, Hantao Ji, H. Akao, K. Akaishi, T. Ono, H. Kaneko, T. Kawamura, Y. Kubota, S. Morimoto. A. Sagara, T. Watanabe, K. Yamazaki and O. Motojima, *Helical Divertor in the Large Helical Device;* May 1992

NIFS-145 K. Ohkubo and K. Matsumoto, *Coupling to the Lower Hybrid Waves with the Multijunction Grill*; May 1992

NIFS-146 K. Itoh, S. -I.Itoh, A. Fukuyama, S. Tsuji and Allan J. Lichtenberg, *A Model of Major Disruption in Tokamaks*; May 1992

NIFS-147 S. Sasaki, S. Takamura, M. Ueda, H. Iguchi, J. Fujita and K. Kadota, *Edge Plasma Density Reconstruction for Fast Monoenergetic Lithium Beam Probing*; May 1992

NIFS-148 N. Nakajima, C. Z. Cheng and M. Okamoto, *High-n Helicity-induced Shear Alfvén Eigenmodes*; May 1992

NIFS-149 A. Ando, Y. Takeiri, O. Kaneko, Y. Oka, M. Wada, and T. Kuroda, *Production of Negative Hydrogen Ions in a Large Multicusp Ion Source with Double-Magnetic Filter Configuration*; May 1992

NIFS-150 N. Nakajima and M. Okamoto, *Effects of Fast Ions and an External Inductive Electric Field on the Neoclassical Parallel Flow, Current, and Rotation in General Toroidal Systems*; May 1992

NIFS-151 Y. Takeiri, A. Ando, O. Kaneko, Y. Oka and T. Kuroda, *Negative Ion Extraction Characteristics of a Large Negative Ion Source with Double-Magnetic Filter Configuration*; May 1992

NIFS-152 T. Tanabe, N. Noda and H. Nakamura, *Review of High Z Materials for PSI Applications* ; Jun. 1992

NIFS-153 Sergey V. Bazdenkov and T. Sato, *On a Ballistic Method for Double Layer Regeneration in a Vlasov-Poisson Plasma*; Jun. 1992

NIFS-154 J. Todoroki, *On the Lagrangian of the Linearized MHD Equations*; Jun. 1992

NIFS-155 K. Sato, H. Katayama and F. Miyawaki, *Electrostatic Potential in a Collisionless Plasma Flow Along Open Magnetic Field Lines;* Jun. 1992

NIFS-156 O.J.W.F.Kardaun, J.W.P.F.Kardaun, S.-I. Itoh and K. Itoh, *Discriminant Analysis of Plasma Fusion Data*; Jun. 1992

NIFS-157 K. Itoh, S.-I. Itoh, A. Fukuyama and S. Tsuji, *Critical Issues and Experimental Examination on Sawtooth and Disruption Physics*; Jun. 1992

NIFS-158 K. Itoh and S.-I. Itoh, *Transition to H-Mode by Energetic Electrons*; July 1992

NIFS-159 K. Itoh, S.-I. Itoh and A. Fukuyama, *Steady State Tokamak Sustained by Bootstrap Current Without Seed Current*; July 1992

NIFS-160 H. Sanuki, K. Itoh and S.-I. Itoh, *Effects of Nonclassical Ion Losses on Radial Electric Field in CHS Torsatron/Heliotron*; July 1992

NIFS-161 O. Motojima, K. Akaishi, K. Fujii, S. Fujiwaka, S. Imagawa, H. Ji,

H. Kaneko, S. Kitagawa, Y. Kubota, K. Matsuoka, T. Mito, S. Morimoto, A. Nishimura, K. Nishimura, N. Noda, I. Ohtake, N. Ohyabu, S. Okamura, A. Sagara, M. Sakamoto, S. Satoh, T. Satow, K. Takahata, H. Tamura, S. Tanahashi, T. Tsuzuki, S. Yamada, H. Yamada, K. Yamazaki, N. Yanagi, H. Yonezu, J. Yamamoto, M. Fujiwara and A. Iiyoshi, *Physics and Engineering Design Studies on Large Helical Device*; Aug. 1992

NIFS-162 V. D. Pustovitov, *Refined Theory of Diamagnetic Effect in Stellarators;* Aug. 1992

NIFS-163 K. Itoh, *A Review on Application of MHD Theory to Plasma Boundary Problems in Tokamaks*; Aug. 1992

NIFS-164 Y.Kondoh and T.Sato, *Thought Analysis on Self-Organization Theories of MHD Plasma*; Aug. 1992

NIFS-165 T. Seki, R. Kumazawa, T. Watari, M. Ono, Y. Yasaka, F. Shimpo, A. Ando, O. Kaneko, Y. Oka, K. Adati, R. Akiyama, Y. Hamada, S. Hidekuma, S. Hirokura, K. Ida, A. Karita, K. Kawahata, Y. Kawasumi, Y. Kitoh, T. Kohmoto, M. Kojima, K. Masai, S. Morita, K. Narihara, Y. Ogawa, K. Ohkubo, S. Okajima, T. Ozaki, M. Sakamoto, M. Sasao, K. Sato, K. N. Sato, H. Takahashi, Y. Taniguchi, K. Toi and T. Tsuzuki, *High Frequency Ion Bernstein Wave Heating Experiment on JIPP T-IIU Tokamak*; Aug. 1992

NIFS-166 Vo Hong Anh and Nguyen Tien Dung, *A Synergetic Treatment of the Vortices Behaviour of a Plasma with Viscosity*; Sep. 1992

NIFS-167 K. Watanabe and T. Sato, *A Triggering Mechanism of Fast Crash in Sawtooth Oscillation*; Sep. 1992

NIFS-168 T. Hayashi, T. Sato, W. Lotz, P. Merkel, J. Nührenberg, U. Schwenn and E. Strumberger, *3D MHD Study of Helias and Heliotron;* Sep. 1992

NIFS-169 N. Nakajima, K. Ichiguchi, K. Watanabe, H. Sugama, M. Okamoto, M. Wakatani, Y. Nakamura and C. Z. Cheng, *Neoclassical Current and Related MHD Stability, Gap Modes, and Radial Electric Field Effects in Heliotron and Torsatron Plasmas;* Sep. 1992

NIFS-170 H. Sugama, M. Okamoto and M. Wakatani, *K- ε Model of Anomalous Transport in Resistive Interchange Turbulence* ; Sep, 1992

NIFS-171 H. Sugama, M. Okamoto and M. Wakatani, *Vlasov Equation in the Stochastic Magnetic Field* ; Sep. 1992

NIFS-172 N. Nakajima, M. Okamoto and M. Fujiwara, *Physical Mechanism of E*

ψ*-Driven Current in Asymmetric Toroidal Systems* ; Sep.1992

NIFS-173 N. Nakajima, J. Todoroki and M. Okamoto, *On Relation between Hamada and Boozer Magnetic Coordinate System* ; Sep. 1992

NIFS-174 K. Ichiguchi, N. Nakajima, M. Okamoto, Y. Nakamura and M. Wakatani, *Effects of Net Toroidal Current on Mercier Criterion in the Large Helical Device* ; Sep. 1992

NIFS-175 S. -I. Itoh, K. Itoh and A. Fukuyama, *Modelling of ELMs and Dynamic Responses of the H-Mode* ; Sep. 1992

NIFS-176 K. Itoh, S.-I. Itoh, A. Fukuyama, H. Sanuki, K. Ichiguchi and J. Todoroki, *Improved Models of* β*-Limit, Anomalous Transport and Radial Electric Field with Loss Cone Loss in Heliotron / Torsatron* ; Sep. 1992

NIFS-177 N. Ohyabu, K. Yamazaki, I. Katanuma, H. Ji, T. Watanabe, K. Watanabe, H. Akao, K. Akaishi, T. Ono, H. Kaneko, T. Kawamura, Y. Kubota, N. Noda, A. Sagara, O. Motojima, M. Fujiwara and A. Iiyoshi, *Design Study of LHD Helical Divertor and High Temperature Divertor Plasma Operation* ; Sep. 1992

NIFS-178 H. Sanuki, K. Itoh and S.-I. Itoh, *Selfconsistent Analysis of Radial Electric Field and Fast Ion Losses in CHS Torsatron / Heliotron* ; Sep. 1992

NIFS-179 K. Toi, S. Morita, K. Kawahata, K. Ida, T. Watari, R. Kumazawa, A. Ando, Y. Oka, K. Ohkubo, Y. Hamada, K. Adati, R. Akiyama, S. Hidekuma, S. Hirokura, O. Kaneko, T. Kawamoto, Y. Kawasumi, M. Kojima, T. Kuroda, K. Masai, K. Narihara, Y. Ogawa, S. Okajima, M. Sakamoto, M. Sasao, K. Sato, K. N. Sato, T. Seki, F. Shimpo, S. Tanahashi, Y. Taniguchi, T. Tsuzuki, *New Features of L-H Transition in Limiter H-Modes of JIPP T-IIU* ; Sep. 1992

NIFS-180 H. Momota, Y. Tomita, A. Ishida, Y. Kohzaki, M. Ohnishi, S. Ohi, Y. Nakao and M. Nishikawa, *D-*^{3}*He Fueled FRC Reactor "Artemis-L"* ; Sep. 1992

NIFS-181 T. Watari, R. Kumazawa, T. Seki, Y. Yasaka, A. Ando, Y. Oka, O. Kaneko, K. Adati, R. Akiyama, Y. Hamada, S. Hidekuma, S. Hirokura, K. Ida, K. Kawahata, T. Kawamoto, Y. Kawasumi, S. Kitagawa, M. Kojima, T. Kuroda, K. Masai, S. Morita, K. Narihara, Y. Ogawa, K. Ohkubo, S. Okajima, T. Ozaki, M. Sakamoto, M. Sasao, K. Sato, K. N. Sato, F. Shimpo, H. Takahashi, S. Tanahasi, Y. Taniguchi, K. Toi, T. Tsuzuki and M. Ono, *The New Features of Ion Bernstein Wave Heating in JIPP T-IIU Tokamak*; Sep, 1992